

Supporting Information

Reactive Oxygen Species Nanoamplifiers with Multi-Enzymatic Activities for Enhanced Tumor Therapy

Shasha Zhao[#], Kexin Lai[#], Zhen Gao, Xueli Ye, Juan Mou, Shiping Yang, and Huixia Wu*

The Education Ministry Key Lab of Resource Chemistry, Joint International Research Laboratory of Resource Chemistry, Ministry of Education, Shanghai Key Laboratory of Rare Earth Functional Materials, Shanghai Municipal Education Committee Key Laboratory of Molecular Imaging Probes and Sensors, and Shanghai Frontiers Science Center of Biomimetic Catalysis, College of Chemistry and Materials Science, Shanghai Normal University, Shanghai 200234, China.

*Email: wuhuixia@shnu.edu.cn

[#]These authors contributed equally to this work.

S1. Experimental Section

1. Chemicals and Reagents. *Ethanol, ammonia, Ce(Ac)₃·H₂O, titanous sulfate, hydrogen peroxide (H₂O₂), methylene blue (MB) and 2, 7-dichlorofluorescein diacetate (DCFH-DA) were purchased from Adamas. Tetramethylbenzidine (TMB) was obtained from Shanghai Macklin Biochemical Co., Ltd. Tetraethyl protosilicate (TEOS) and sodium triacetate (NaAc·3H₂O) were provided by Shanghai Titan Technology Co., Ltd. mPEG-Silane was obtained from Achem-block. Saikosaponin A (SSA) was purchased from Shanghai yuanye Bio-Technology Co., Ltd. 5, 5'-Dithiobis-(2-nitrobenzoic acid) (DTNB) was provided by Aladdin Reagents, Ltd. Dihydroethidium (DHE) was obtained from Sigma-Aldrich. Calcein acetoxymethyl ester (Calcein-AM) / propidium iodide (PI) cell viability / cytotoxicity assay kit, methylthiazolyldiphenyl-tetrazolium bromide (MTT), 4', 6-diamidino-2-phenylindole (DAPI) staining solution and mitochondrial membrane potential assay kit with JC-1 were supplied by Shanghai Beyotime Biotechnology Co., Ltd. Deionized (DI) water with a resistivity higher than 18 MΩ cm was used in all experiments.*

2. Characterizations. *Scanning electron microscopy (SEM) images were obtained from a Hitachi S-4800 microscope. Transmission electron microscopy (TEM) images and elemental mapping images were taken by a field emission transmission electron microscope (JEOL JEM-2199 and JEOL JEM-2100F), respectively. X-ray photoelectron spectroscopy (XPS) spectra were collected on an AXIS-165 instrument. X-ray diffraction (XRD) patterns were acquired from a Rigaku DMAX 2000 diffractometer. Dynamic light scattering (DLS) and Zeta potential measurements were performed on a Zetasizer Nano ZS90 analyzer (Malvern). Fourier transform infrared (FTIR) spectra were recorded on a FTIR spectrophotometer (Nicolet Avatar 370). The nitrogen (N₂) adsorption-desorption isotherm and corresponding pore size distribution were determined by the Micromeritics Tristar II 3020 system. The*

Brunauer-Emmett-Teller (BET) method was employed to determine the surface area of each sample. UV-vis absorption spectra were performed on a UV-vis spectrophotometer (BeckMan coulter DU 730). Fluorescence spectra were measured on a fluorescent spectrometer (Cary Eclipse). Fluorescence images were obtained from a confocal laser scanning microscopy (CLSM) instrument (Leica TCS SP5).

3. Synthesis of SiO₂ Nanoparticles. *50 mL of ethanol and 2.5 mL of ammonia were mixed with 1.5 mL of water and heated at 70 °C in a water bath. Then, 1.9 mL of TEOS was added into the mixture via the syringe pump in nearly 2.5 h. The mixed solution was vigorously stirred and reacted at 70 °C for 4 h. After the reaction, the mixture was centrifuged and the collected product was washed with ethanol and water. Finally, the resulting solid was dispersed in water.*

4. Synthesis of Ce-doped hollow mesoporous silica nanoparticles (Ce-HMSNs). *Ce-HMSNs were prepared through a hydrothermal process. 1 mmol of Ce(Ac)₃·H₂O and 900 mg of NaAc·3H₂O were dissolved in 10 mL of water. Then, 20 mg of SiO₂ nanoparticles were dispersed in another 10 mL of water. The two solutions were mixed together uniformly and then transferred into a tetrafluoroethylene vessel, which was sealed in a stainless-steel autoclave. The autoclave was heated at 180 °C for 4 h. After natural cooling to room temperature, the mixture was centrifuged. The obtained solid was washed with water for three times and finally dispersed in water for later use.*

5. Synthesis of Ce-HMSN-PEG. *10 mg of Ce-HMSNs were dispersed in 10 mL of water. Then, 30 mg of mPEG-Silane was added into the dispersion. The mixture was stirred at room temperature (25 °C) in dark for 24 h. After the reaction, the solution was centrifuged and the obtained solid was washed three times with water. Finally, the resulting Ce-HMSN-PEG was dispersed in water.*

6. Preparation of SSA@Ce-HMSN-PEG. For drug loading, 4 mg of SSA was added into a 10 mL aqueous dispersion of 10 mg Ce-HMSN-PEG. The mixed solution was vigorously stirred (600 rpm/min) and incubated at room temperature (25 °C) in dark for 24 h. After that, the mixture was centrifuged. The obtained solid was washed twice with water and then dispersed in water, obtaining the aqueous solution of SSA@Ce-HMSN-PEG.

7. Release of Ce Ions. The release of Ce ions after incubation of Ce-HMSNs under different conditions was assessed with inductively coupled plasma-atomic emission spectrometry (ICP-AES). Four groups were allocated as (1) pH 7.4, (2) pH 6.5, (3) pH 5.2 and (4) pH 5.2 + 5 mM GSH. Ce-HMSNs were diluted in phosphate-buffered saline (PBS) solution (500 $\mu\text{g mL}^{-1}$, 10 mL) and packed into dialysis bags (MWCO = 3500 Da), which were then immersed in 20 mL of corresponding buffer at 37 °C. The dialysate (3 mL) was removed at different time points for ICP-AES detection. Meanwhile, an equal volume of fresh buffer was added to the solution outside the dialysis bags.

8. In Vitro Degradation Observation. SEM was employed to compare the morphology change of Ce-HMSNs after incubation for 6 h under different conditions. This experiment involves six groups. Ce-HMSNs (200 $\mu\text{g mL}^{-1}$) were allowed to incubate under the following conditions: (1) pH 7.4, (2) pH 6.5, (3) pH 5.2, (4) pH 7.4 + 5 mM GSH, (5) pH 6.5 + 5 mM GSH and (6) pH 5.2 + 5 mM GSH.

9. O₂ Generation Measurement. The dissolved oxygen level was monitored in real time using a dissolved oxygen meter. Five groups were allocated as: (1) pH 7.4 + 10 mM H₂O₂, (2) pH 7.4 + 200 $\mu\text{g mL}^{-1}$ Ce-HMSNs, (3) pH 7.4 + 200 $\mu\text{g mL}^{-1}$ Ce-HMSNs + 10 mM H₂O₂, (4) pH 6.5 + 200 $\mu\text{g mL}^{-1}$ Ce-HMSNs + 10 mM H₂O₂ and (5) pH 5.2 + 200 $\mu\text{g mL}^{-1}$ Ce-HMSNs + 10 mM H₂O₂. The concentrations of dissolved oxygen were recorded every 5 min, and the total monitoring time was 60 min.

10. H₂O₂ Depletion Ability Assessment. *H₂O₂ depletion ability was measured by the titanium sulfate (Ti(SO₄)₂) spectrophotometric method. Titanium ions (Ti⁴⁺) in acidic medium can react with H₂O₂ to form an orange complex, which exhibits a characteristic absorption peak at 405 nm.*

Preparation of Ti(SO₄)₂-H₂SO₄ mixed indicator: 960 mg of Ti(SO₄)₂ was dissolved in 20 mL of water, obtaining the Ti(SO₄)₂ aqueous solution (4.8%). After that, 333 μL of concentrated H₂SO₄ was added dropwise into 266 μL of the Ti(SO₄)₂ aqueous solution.

Plotting of standard H₂O₂ curve: A series of standard H₂O₂ solutions were prepared and the concentrations were set to 0.05, 0.1, 0.2, 0.5, 1, 1.5, 2, 2.5 and 3 mM. Then, the standard H₂O₂ solutions were mixed uniformly with the Ti(SO₄)₂-H₂SO₄ indicator (the total volume = 2 mL). After the reaction was proceeded for 5 min, the absorption spectra of the solutions in the range of 300–600 nm were measured. As a result, standard H₂O₂ curve was plotted according to the absorbance at λ = 405 nm.

The depletion ability of Ce-HMSNs with various concentrations on 1 mM of H₂O₂: Ce-HMSNs (0, 50, 100 and 200 μg mL⁻¹) were mixed uniformly with 1 mM of H₂O₂ and then incubated at 37 °C for 1 h. After the reaction, the Ti(SO₄)₂-H₂SO₄ indicator was then added to reach a total volume of 2 mL and the absorption spectra of the solutions in the range of 300–600 nm were measured.

The maximum H₂O₂ depletion of Ce-HMSNs: Ce-HMSNs (200 μg mL⁻¹) was incubated with H₂O₂ (1, 2, 4, 6, 8 and 10 mM) at 37 °C for 1 h. After that, the Ti(SO₄)₂-H₂SO₄ indicator was added (the total volume = 2 mL), and the absorption spectra of the solutions were measured.

11. GSH Consumption Assay. *DTNB was used as the indicator to assess the GSH depletion ability of Ce-HMSNs. Ce-HMSNs (200, 300 or 400 μg mL⁻¹) were added into the PBS*

solutions (pH 7.4, 6.5 or 5.2) containing GSH (1 mM or 5 mM) and then incubated at 37 °C for 2 or 12 h. The supernatant (200 μ L) was diluted to 2 mL with the PBS solution (pH 7.4). After adding the DTNB solution (100 mM, 10 μ L), the absorbance of the solution within the range of 400–600 nm was recorded using UV-vis spectroscopy.

12. POD-Mimic Catalytic Activity Measurement by TMB. *Ce-HMSNs* (200 μ g mL⁻¹) were dispersed in the PBS solutions (pH 6.5 or 7.4). Then, 0.8 mM TMB and 1 mM H₂O₂ were added into the solutions. The absorbance of the mixed solutions in the range of 500–800 nm after different reaction times was measured using UV-vis spectroscopy.

13. Hydroxyl Radical Generation Capacity. Briefly, 10 μ g mL⁻¹ of MB and 1 mM of H₂O₂ were added into the PBS suspension of *Ce-HMSNs* (200 μ g mL⁻¹, pH = 5.2, 6.5 or 7.4) with or without GSH (1 mM). At different time points after the start of the reaction, the absorbance of the solutions in the range of 550–750 nm was measured using UV-vis spectroscopy.

14. Drug Release. To investigate the pH- and GSH-triggered SSA release behaviors of SSA@*Ce-HMSN-PEG*, four groups were allocated as (1) pH 7.4, (2) pH 6.5, (3) pH 5.2 and (4) pH 5.2 + 5 mM GSH. SSA@*Ce-HMSN-PEG* was diluted in phosphate-buffered saline (PBS) solution (600 μ g mL⁻¹, 10 mL), packed into dialysis bag (MWCO = 3,500 Da) and then dialyzed against 20.0 mL of corresponding buffer in a shaking bed (110 rpm min⁻¹, 37 °C). At different time intervals (2, 6, 12 and 24 h), 3.0 mL of PBS solution was taken out. At the same time, 3.0 mL fresh PBS solution was added to keep the same total volume. The amount of released SSA at different times was calculated by testing the UV absorbance of the SSA at 210 nm. All experiments were done in triplicate.

15. Cell Culture. 4T1 cells and Human Umbilical Vein Endothelial cells (HUVECs) were obtained from Fudan University Shanghai Cancer Center. 4T1 cells were cultured with Roswell Park Memorial Institute (RPMI) 1640 containing 1% antibiotics mixture (penicillin-

streptomycin) and 10% fetal bovine serum (FBS) at 37 °C under 5% CO₂. The medium used for incubating HUVECs was Dulbecco's modified Eagle medium (DMEM) and other incubation conditions were the same as those of 4T1 cells.

16. In Vitro Cytotoxicity. *Three groups were allocated as (1) SSA, ([SSA] = 0, 5, 10, 20, 30, 40 μM), (2) Ce-HMSN-PEG, ([Ce] = 0, 0.1, 0.2, 0.4, 0.6, 0.8 mM) and (3) SSA@Ce-HMSN-PEG, ([Ce] = 0, 0.1, 0.2, 0.4, 0.6, 0.8 mM, [SSA] = 0, 5, 10, 20, 30, 40 μM). HUVECs were seeded on 96-well plates at a density of 2×10^4 cells per well. After cell adhesion, the cells were incubated with different samples for 12 and 24 h, followed by washing with PBS. Cells in each well was then incubated with 100 μL of fresh MTT solution for 4 h. Finally, dimethyl sulfoxide (DMSO, 150 μL) was added and the absorbance of the solutions at $\lambda = 492$ nm was measured to evaluate the cell viability.*

17. Hemolysis Test. *About 1 mL of fresh mouse blood collected from the mouse eyeballs was mixed with 9 mL of PBS and then the mixture was centrifuged to remove plasma. The collected red blood cells (RBCs) were washed with PBS for 3 times and diluted with PBS to 12 mL. Then, 400 μL of RBC suspension was incubated with different concentrations (50, 100, 200, 400 and 600 μg mL⁻¹) of SSA@Ce-HMSN-PEG (1mL) at 37 °C for 2 h. The samples were centrifuged, and the absorbance of the supernatants from 500 to 700 nm was measured to evaluate the hemolysis effect. The RBCs in PBS and distilled water without adding SSA@Ce-HMSN-PEG were used as negative control and positive control, respectively.*

18. Calcein-AM/PI Double Staining. *The experiments were divided into seven groups, in which 4T1 cells seeded in CLSM-exclusive cultrue dishes (35 nm) were incubated with the following samples for 6 h: (1) only medium (control group), (2) 0.1 mM H₂O₂, (3) Ce-HMSN-PEG, (4) Ce-HMSN-PEG + 0.1 mM H₂O₂, (5) SSA, (6) SSA@Ce-HMSN-PEG and (7) SSA@Ce-HMSN-PEG + 0.1 mM H₂O₂ ([SSA] = 30 μM, [Ce] = 0.6 mM). After that, the cells*

were co-stained with calcein-AM and PI and finally observed by CLSM (green fluorescence, 488 nm laser, for calcein-AM; red fluorescence, 543 nm laser, for PI). Green and red fluorescence indicate live and dead cells, respectively.

19. Intracellular ROS Detection. *The intracellular ROS level was investigated with DCFH-DA, an oxidation-sensitive fluorescence probe. 4T1 cells were seeded in CLSM-exclusive culture dishes (35 nm) and incubated with different samples for 6 h. Seven groups were allocated as (1) control group, (2) 0.1 mM H₂O₂, (3) Ce-HMSN-PEG, (4) Ce-HMSN-PEG + 0.1 mM H₂O₂, (5) SSA, (6) SSA@Ce-HMSN-PEG and (7) SSA@Ce-HMSN-PEG + 0.1 mM H₂O₂ ([SSA] = 30 μM, [Ce] = 60 mM). Then, the cells were stained with DCFH-DA solution for 30 min and examined by CLSM ($\lambda_{ex} = 488 \text{ nm}$, $\lambda_{em} = 500\text{--}550 \text{ nm}$) to obtain images.*

20. Intracellular •O₂⁻ Detection. *DHE was utilized as a specific superoxide anion (•O₂⁻) indicator in cells. 4T1 cells seeded in CLSM-exclusive culture dishes were incubated with the samples for 6 h. The experiments included following four groups: (1) control group, (2) SSA, (3) Ce-HMSN-PEG and (4) SSA@Ce-HMSN-PEG ([SSA] = 30 μM, [Ce] = 0.6 mM). Then, the DHE solution was added and incubated with the cells for 30 min. Finally, the cells were observed by CLSM ($\lambda_{ex} = 488 \text{ nm}$, $\lambda_{em} = 579\text{--}630 \text{ nm}$).*

21. Intracellular H₂O₂ Detection. *Plotting of standard H₂O₂ curve: A series of standard H₂O₂ solutions were prepared in cell lysis buffer and the concentrations were set to 1, 2, 5, 10, 20 and 50 mM. Then, standard H₂O₂ solutions (the total volume = 50 μL) of various concentrations were added into 96-well plates for 30 min. The absorbance at 560 nm was measured with a microplate reader. Standard H₂O₂ curve was plotted according to the absorbance at $\lambda = 560 \text{ nm}$.*

Measurement of intracellular H₂O₂ level: The SSA solution (20 mM) was prepared in DMSO and diluted to 30 μM with RPMI-1640. Then, 4T1 cells were seeded on 6-well plates

and incubated with the SSA solution (the total volume = 2 mL) for 6 h. The cells were lysed by cell lysis buffer (300 μ L). Supernatant containing H_2O_2 was collected by centrifugation at 12,000 rpm for 5 min. The supernatant (50 μ L) and hydrogen peroxide assay kit (100 μ L) were added into 96-well plates and mixed together uniformly. After the mixtures were allowed to stand for 30 min at room temperature, the absorbance at 560 nm was recorded with the microplate reader.

22. Intracellular O_2 Assay. $Ru(dpp)_3Cl_2$ was used as an oxygen probe to detect intracellular O_2 generation. 4T1 cells were seeded in CLSM-exclusive culture dishes and then incubated with the following samples for 6 h: (1) control group, (2) 0.1 mM H_2O_2 , (3) Ce-HMSN-PEG, (4) Ce-HMSN-PEG + 0.1 mM H_2O_2 , (5) SSA, (6) SSA@Ce-HMSN-PEG and (7) SSA@Ce-HMSN-PEG + 0.1 mM H_2O_2 ([SSA] = 30 μ M, [Ce] = 0.6 mM). Afterwards, the $Ru(dpp)_3Cl_2$ solution (10 μ M, 1 mL) was added and the confocal dishes was sealed with parafilm. After incubation for 30 min, CLSM observation was performed to assess intracellular O_2 production (λ_{ex} = 488 nm, λ_{em} = 550–660 nm).

23. Mitochondrial Membrane Potential Assay. 4T1 cells seeded in CLSM-exclusive culture dishes were incubated with the samples for 6 h. Seven groups were allocated as (1) control group, (2) 0.1 mM H_2O_2 , (3) Ce-HMSN-PEG, (4) Ce-HMSN-PEG + 0.1 mM H_2O_2 , (5) SSA, (6) SSA@Ce-HMSN-PEG and (7) SSA@Ce-HMSN-PEG + 0.1 mM H_2O_2 ([SSA] = 30 μ M, [Ce] = 0.6 mM). Then the JC-1 staining solution was added into the dishes and incubated for 20 min. After washing with JC-1 staining buffer, the cell nuclei were stained with the diluted DAPI staining solution for 15 min. Finally, CLSM was used to assess the changes in mitochondrial membrane potential (JC-1 monomer, λ_{ex} = 514 nm, λ_{em} = 520–550 nm; JC-1 polymer, λ_{ex} = 585 nm, λ_{em} = 590–620 nm).

24. Accumulation in Tumor Tissues. BALB/c female mice (4–5 weeks old) were provided by Shanghai JieSiJie Laboratory Animal Co., Ltd. All animal experiments were approved by the

Experimental Animal Management and Animal Welfare Ethics Committee of Shanghai Normal University, and were carried out in strict accordance with the national and local Guidelines on the Care and Use of Laboratory Animals (China). The tumor model was established by subcutaneously injecting 2×10^5 4T1 cells in 100 μ L PBS into right hindlimb of each mouse. When the tumor volume reached about 100 mm³, SSA@Ce-HMSN-PEG ([SSA] = 1.4 mg kg⁻¹, [Ce] = 5 mg kg⁻¹) was intravenously injected into 4T1 tumor-bearing mice via the caudal vein. At 6, 12 and 24 h (3 mice per group) postinjection, the tumors were harvested, weighed and cut into pieces. After digestion, Ce content in tumor tissues was measured by ICP-AES.

25. In Vivo Antitumor Efficacy. *4T1 tumor-bearing mice with tumor volumes of about 100 mm³ were randomly assigned into five groups (5 mice per group): (1) PBS (100 μ L, control group), (2) SSA ([SSA] = 1.4 mg kg⁻¹, 100 μ L), (3) Ce-HMSN-PEG ([Ce] = 5 mg kg⁻¹, 100 μ L) and (4) SSA@Ce-HMSN-PEG ([SSA] = 1.4 mg kg⁻¹, [Ce] = 5 mg kg⁻¹, 100 μ L). The agents for each group were intravenously injected via the caudal vein on day 0, 4 and 14 (a total of three times). Body weights and tumor volumes of the mice were measured every 2 days. After the last administration on day 14 for 6 h, one mouse in each group was randomly selected and sacrificed, and the tumors were dissected for H&E, TUNEL and DCFH-DA staining as well as HIF-1 α immunofluorescence staining. On day 24, the remaining mice in each group were sacrificed and the tumors were harvested, weighed and photographed. Furthermore, the main organs (heart, liver, spleen, lung and kidney) of the presentative mice from the groups of (1) PBS (control) and (4) SSA@Ce-HMSN-PEG were collected, sectioned and stained with H&E for histopathological evaluation, and the blood samples were also harvested for blood routine and biochemical blood analysis.*

26. Statistical Analysis. *A two-tailed unpaired student's t-test was employed for statistical analysis. The data were expressed as mean \pm standard deviation. * $p < 0.05$ was considered*

*statistically significant. ** $p < 0.01$, *** $p < 0.001$ and **** $p < 0.0001$ were considered extremely significant.*

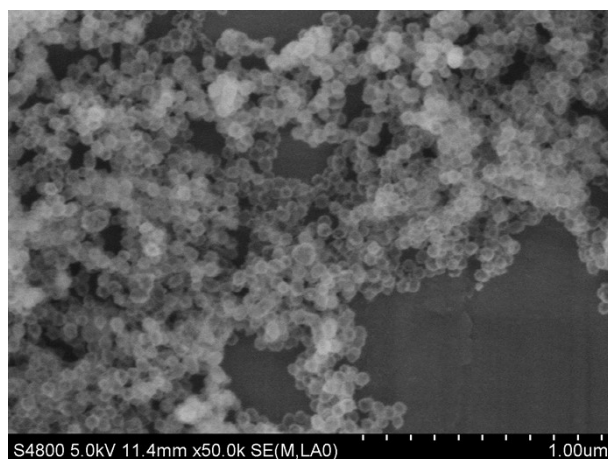


Fig. S1. SEM image of Ce-HMSNs.

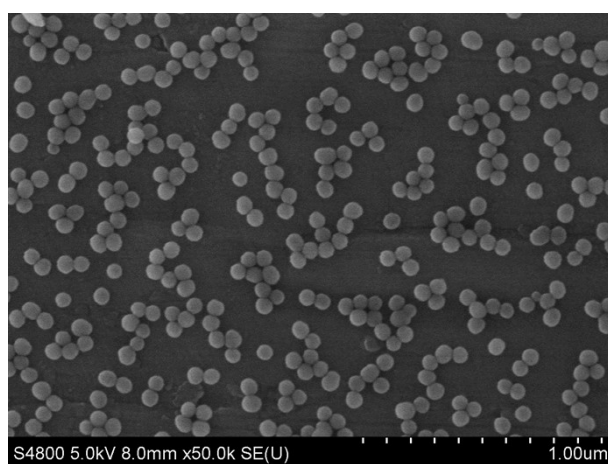


Fig. S2. SEM image of SiO₂ nanoparticles.

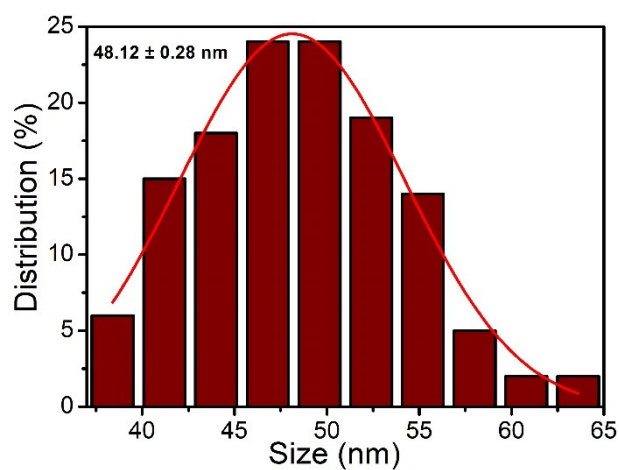


Fig. S3. Particle size distribution of Ce-HMSNs according to TEM images.

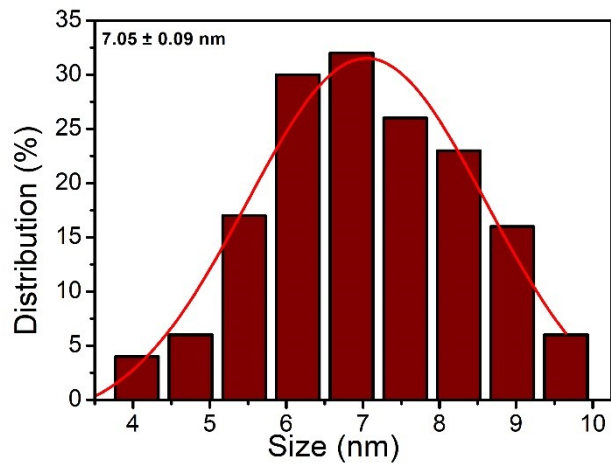


Fig. S4. Shell thickness distribution of Ce-HMSNs according to TEM images.

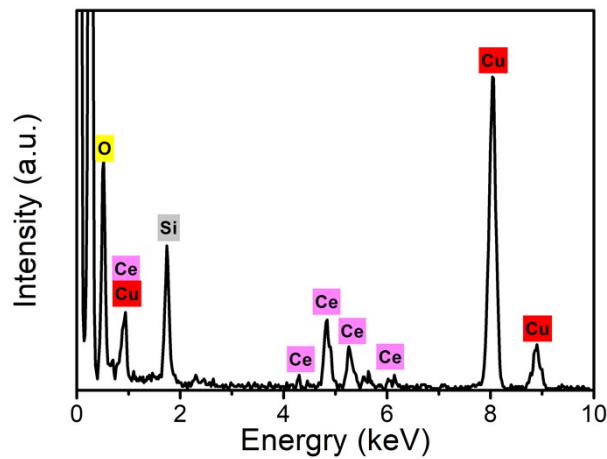


Fig. S5. Energy dispersive spectroscopy (EDS) spectrum of the as-prepared Ce-HMSNs.

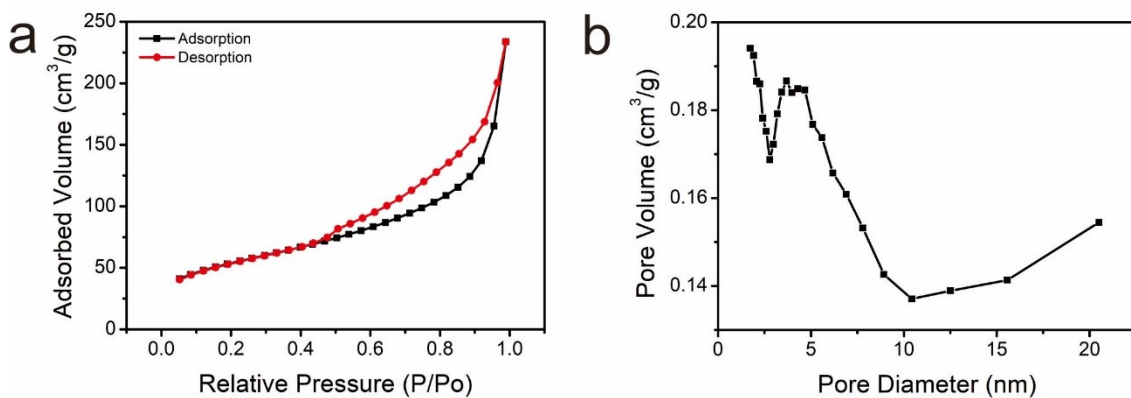


Fig. S6. (a) Nitrogen adsorption-desorption isothermal curves and (b) Corresponding aperture distribution of Ce-HMSNs.

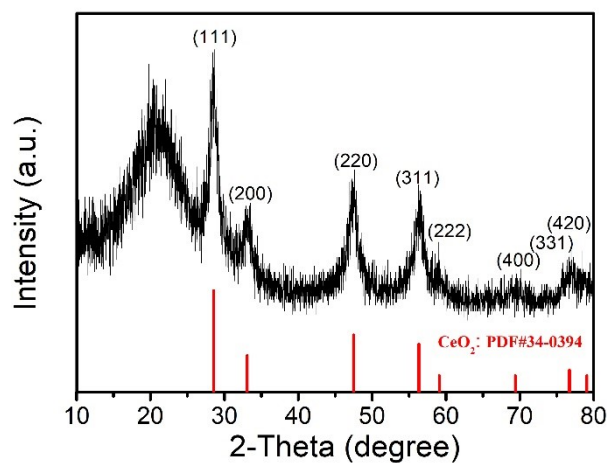


Fig. S7. XRD pattern of Ce-HMSNs and standard peak positions.

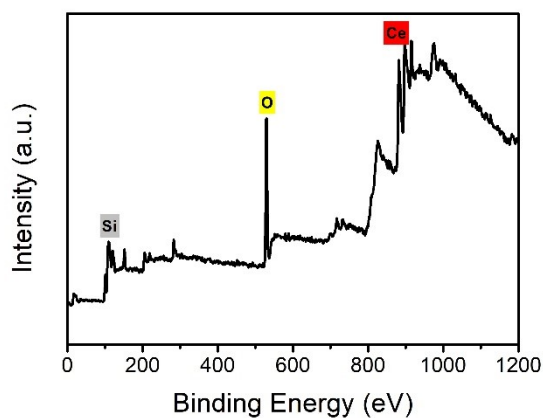


Fig. S8. XPS spectrum of Ce-HMSNs.

Table S1. Binding energy data of Ce obtained from Ce 3d regions of Ce-HMSNs.

	Ce ³⁺			Ce ⁴⁺	
	v ₀	v'	v	v''	v'''
Ce(3d _{5/2})	880	884.8	882.6	889.3	899.5
	u ₀	u'	u	u''	u'''
Ce(3d _{3/2})	889.5	903	900.8	907.8	916.7

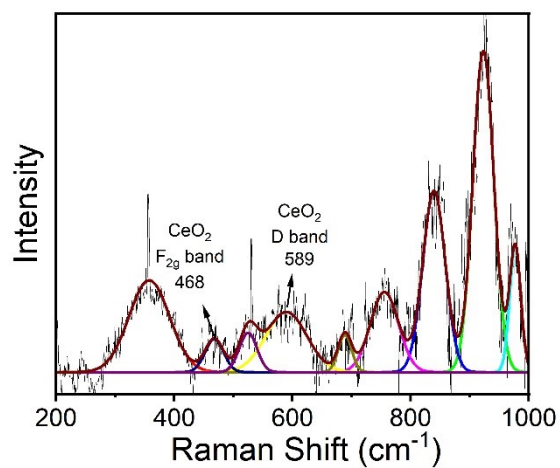


Fig. S9. Raman spectrum of Ce-HMSNs.

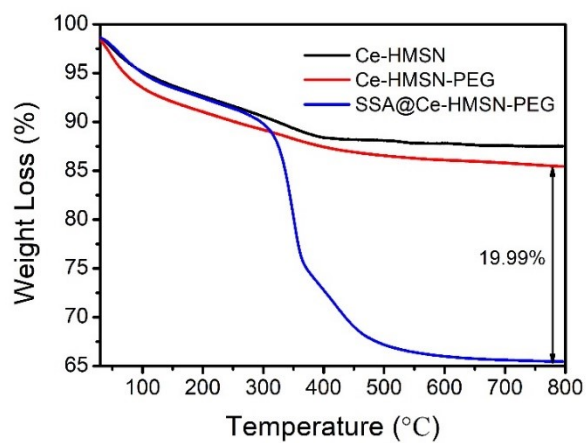


Fig. S10. Thermogravimetry analysis (TGA) curves of Ce-HMSNs, Ce-HMSN-PEG and SSA@Ce-HMSN-PEG.

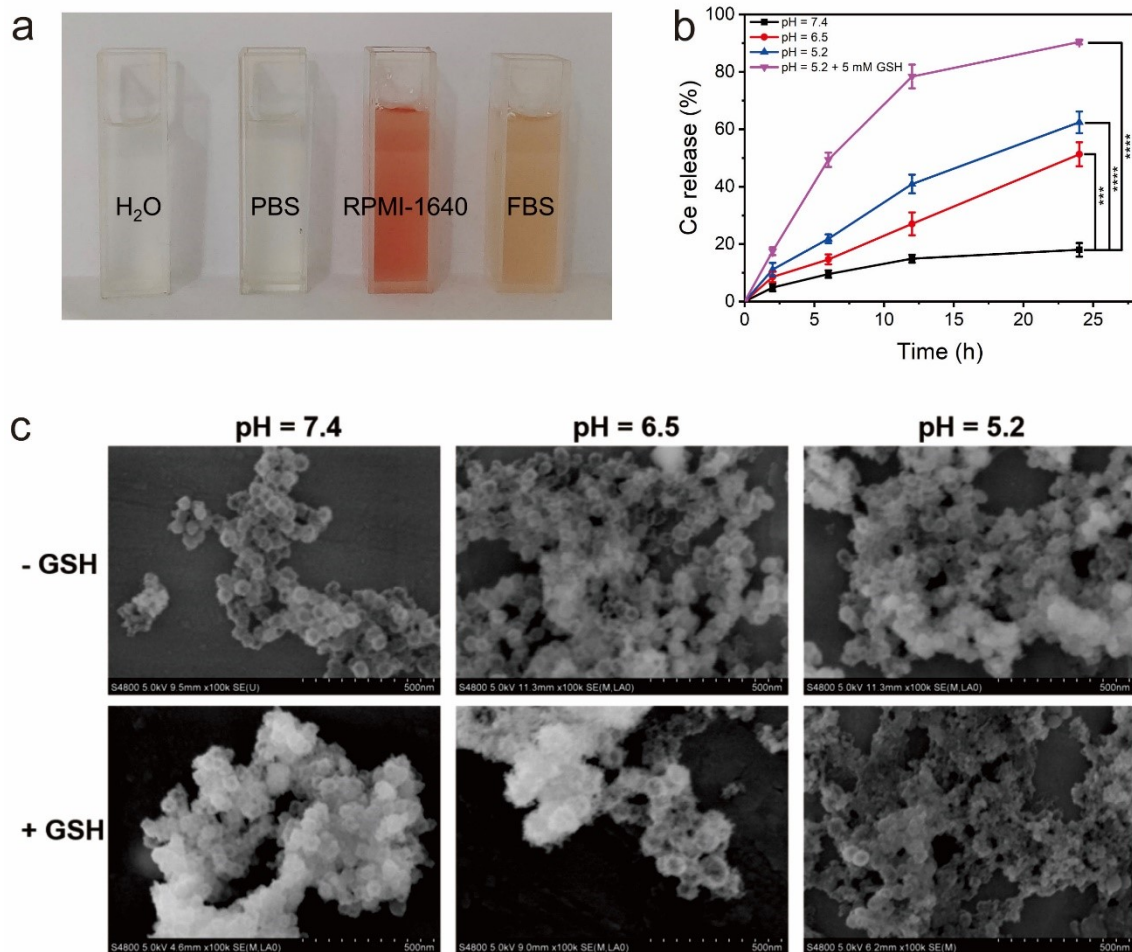


Fig. S11. (a) The photograph taken after SSA@Ce-HMSN-PEG was dispersed in H₂O, PBS, RPMI-1640 and FBS for 12 h, respectively. (b) Release curves of Ce ions from Ce-HMSNs at different pH values with or without GSH (***p* < 0.001; *****p* < 0.0001). (c) SEM images of Ce-HMSNs after 6 h of incubation at different pH values with or without GSH.

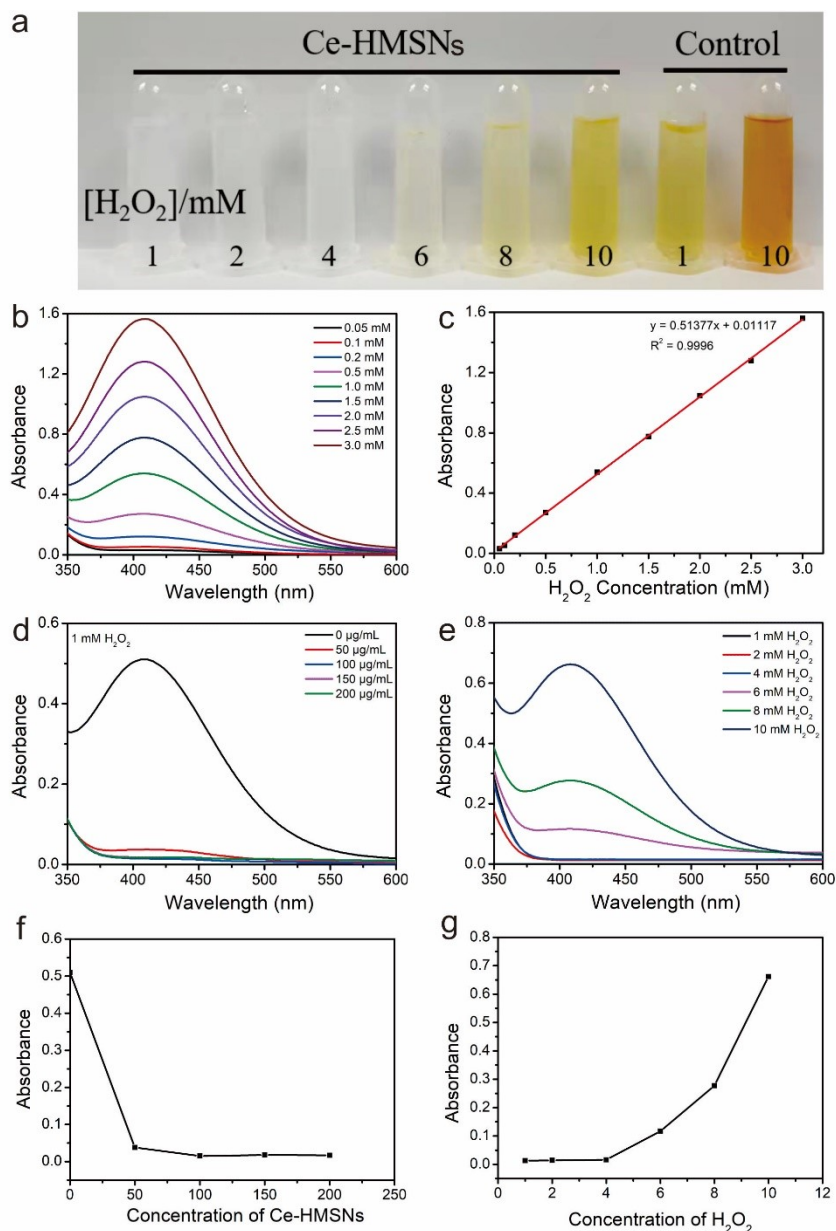


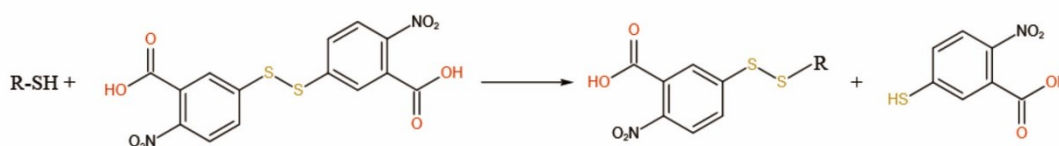
Fig. S12. In vitro evaluation of H₂O₂ depletion performance of Ce-HMSNs. (a) The photograph of chromogenic reaction to detect the remaining H₂O₂ after Ce-HMSNs (200 µg mL⁻¹) were mixed with various concentrations of H₂O₂. (b) Absorption spectra of H₂O₂-Ti(SO₄)₂ solutions with various H₂O₂ concentrations. (c) Standard curve of H₂O₂. (d) Absorption spectra of H₂O₂-Ti(SO₄)₂ solutions after H₂O₂ (1 mM) was incubated with various concentrations of Ce-HMSNs. (e) Absorption spectra of H₂O₂-Ti(SO₄)₂ solutions after Ce-HMSNs (200 µg mL⁻¹) were treated with various concentrations of H₂O₂. (f) Quantitative analysis of the maximum absorption peak from Fig. S12d. (g) Quantitative analysis of the maximum absorption peak from Fig. S12e.

pH = 7.4 6.5 5.2

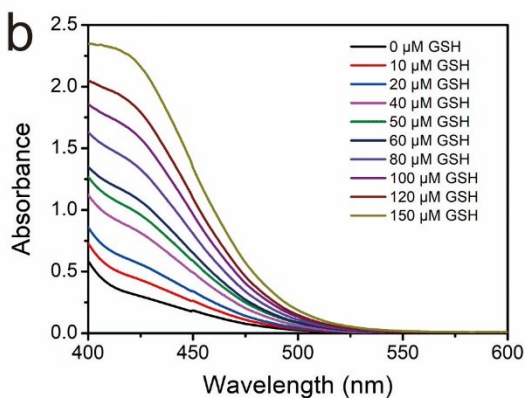


Fig. S13. The photograph for observation of oxygen generation in the mixed solutions of Ce-HMSNs (200 μg mL⁻¹) and H₂O₂ (10 mM) at pH 7.4, 6.5 and 5.2.

a



b



c

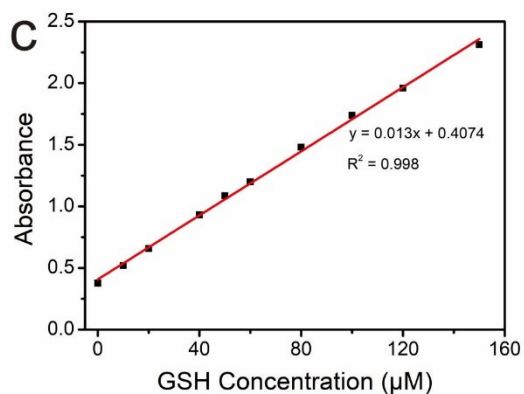


Fig. S14. (a) Detection mechanism of DTNB on GSH. (b) Absorption spectra of the solutions of DTNB mixed with different concentrations of GSH. (c) Standard curve of GSH.

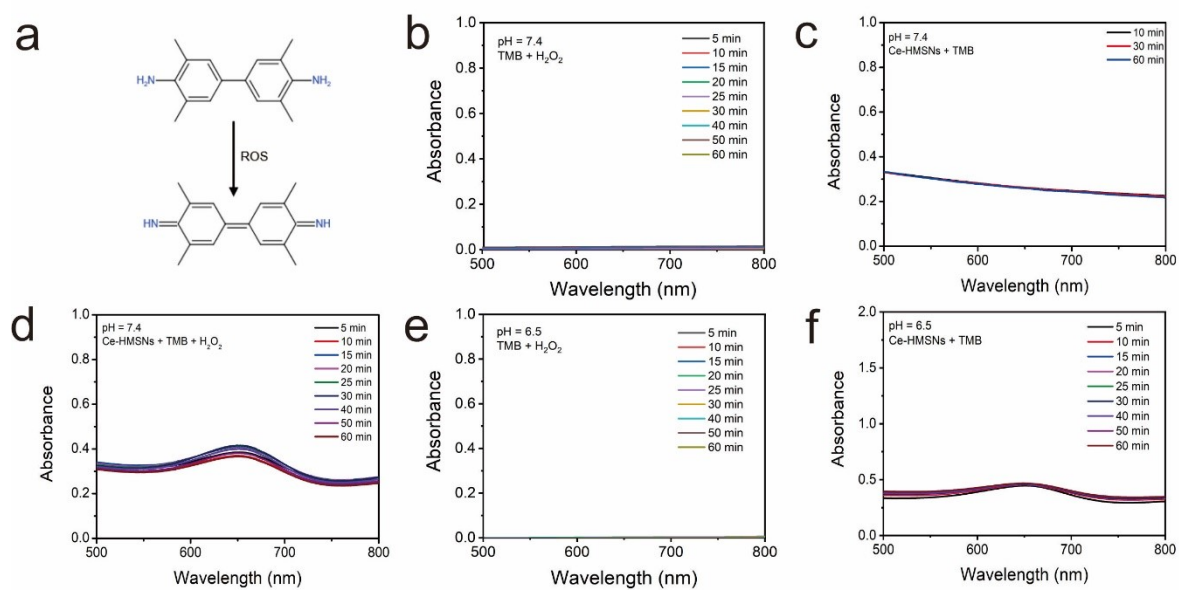


Fig. S15. (a) Detection mechanism of TMB on ROS. Absorption spectra to assess the oxidation of TMB in the PBS solutions of (b) H_2O_2 (pH 7.4), (c) Ce-HMSNs (pH 7.4), (d) Ce-HMSNs + H_2O_2 (pH 7.4), (e) H_2O_2 (pH 6.5) and (f) Ce-HMSNs (pH 6.5).

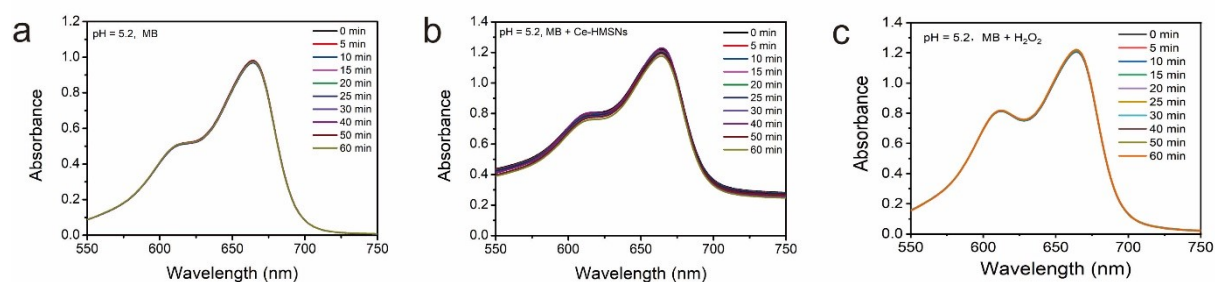


Fig. S16. Absorption spectra for $\cdot\text{OH}$ generation detection using MB as the probe under the conditions of (a) MB, (b) MB + Ce-HMSNs and (c) MB + H_2O_2 at pH = 5.2.

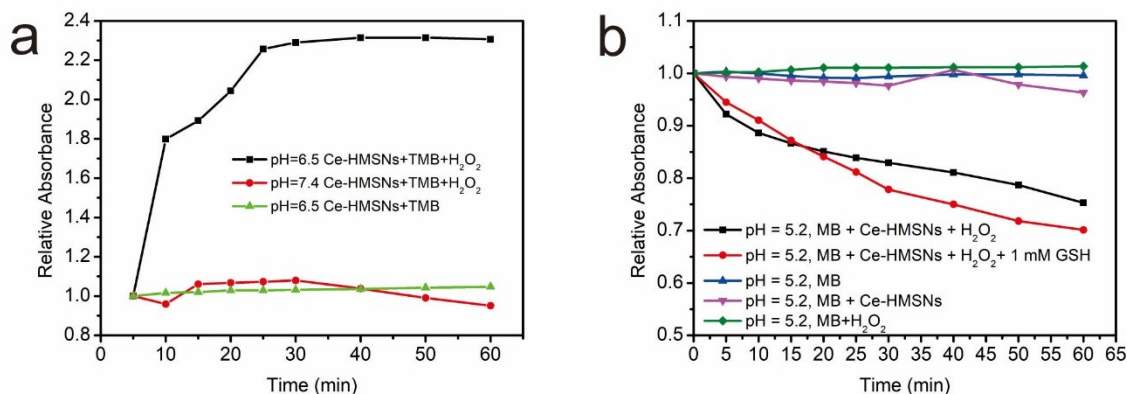


Fig. S17. (a) Quantitative analysis of the normalized maximum absorption peak to assess the oxidation of TMB from Fig. 2f, Fig. S15d and Fig. S15f. (b) Quantitative analysis of the normalized maximum absorption peak for \bullet OH generation detection using MB as the probe from Fig. 2g, Fig. 2h and Fig. S16.

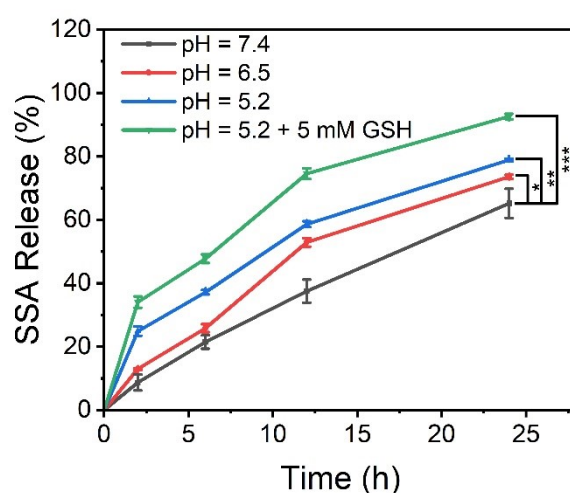


Fig. S18. *In vitro* drug-release profile of SSA@Ce-HMSNs-PEG at different pH values with or without GSH (* $p < 0.05$; ** $p < 0.01$; *** $p < 0.001$).

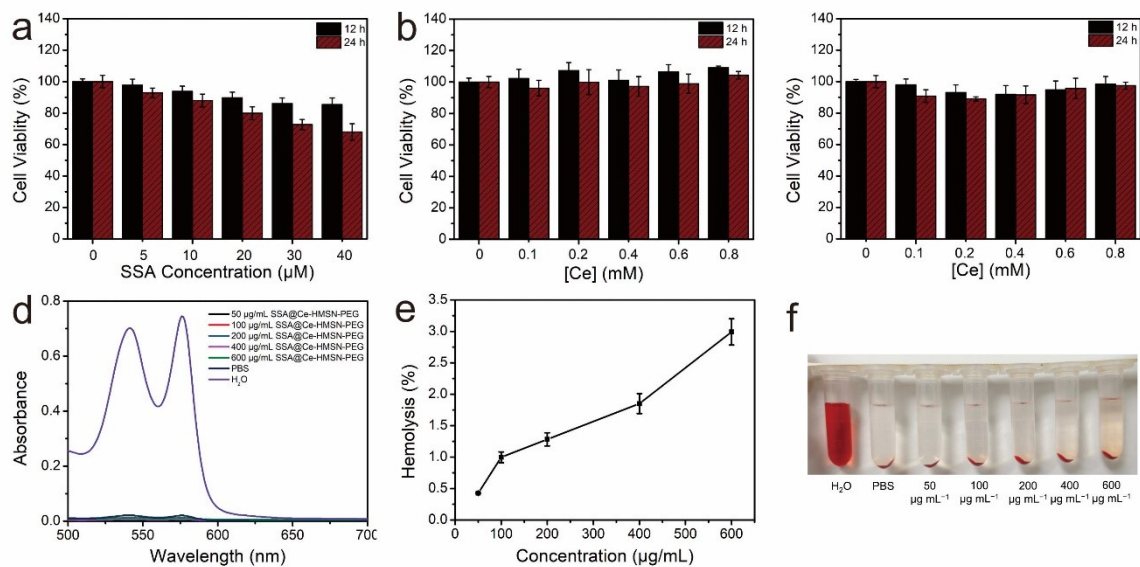


Fig. S19. Viability of HUVECs cultured with different concentrations of SSA (a), Ce-HMSN-PEG (b) and SSA@Ce-HMSN-PEG (c) for 12 and 24 h. (d) Absorption profiles of the supernatants obtained after treatment of the red blood cells with different concentrations of SSA@Ce-HMSN-PEG. (e) Hemolysis of SSA@Ce-HMSN-PEG with various concentrations using water and PBS as the positive and negative control, respectively. (f) The corresponding picture of hemolysis induced by SSA@Ce-HMSN-PEG with various concentrations.

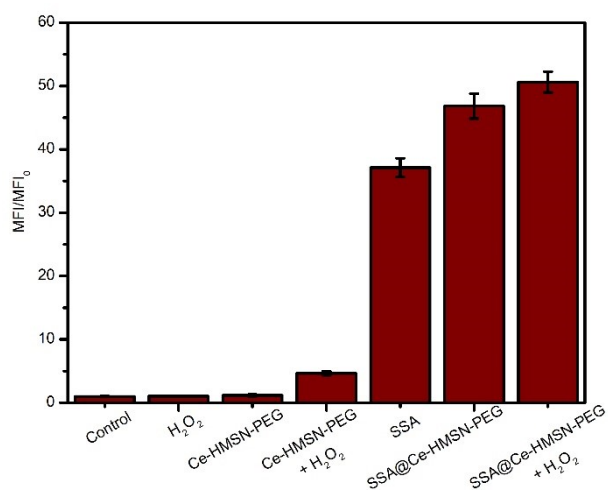


Fig. S20. Mean fluorescence intensity (MFI) of DCF in different treatment groups, which corresponds to Fig. 3c2.

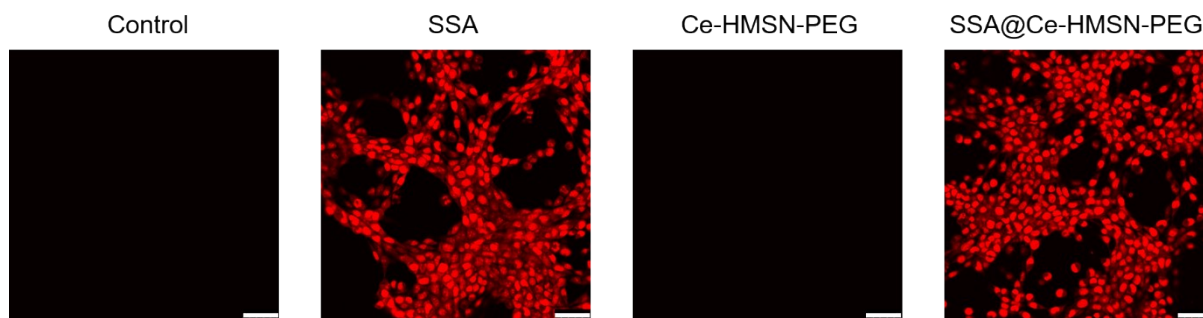


Fig. S21. Confocal microscopy images of different treatment groups using DHE as the fluorescence probe to detect the generation of $\bullet\text{O}_2^-$. Scale bar: 50 μm .

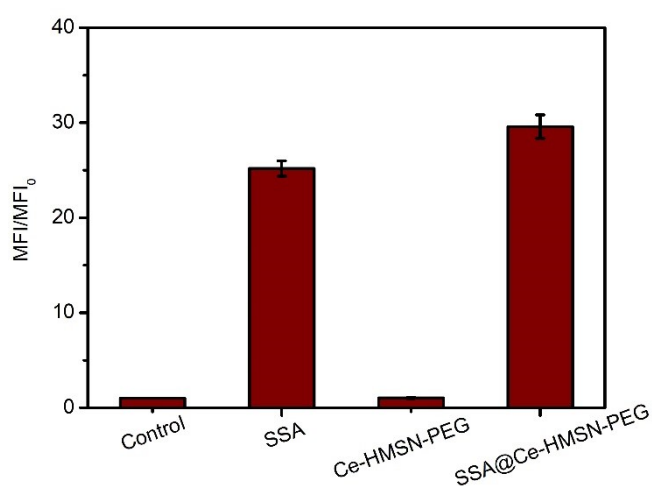


Fig. S22. MFI of DHE in different treatment groups, which corresponds to Fig. S20.

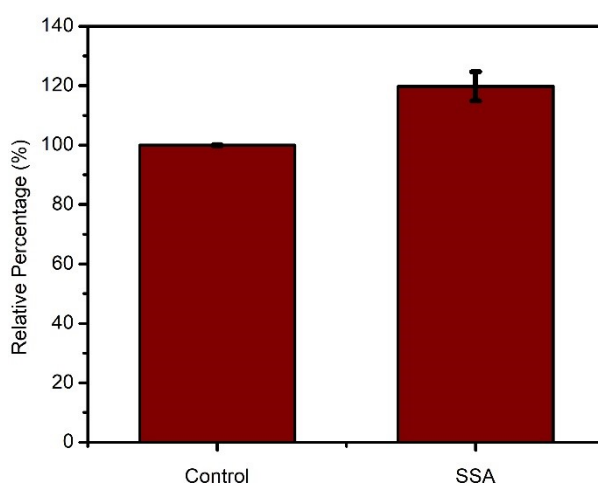


Fig. S23. Intracellular H_2O_2 content in 4T1 cells after being treated with SSA.

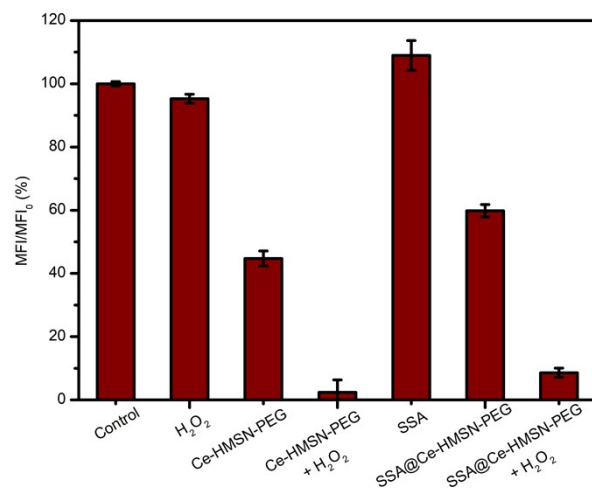


Fig. S24. Relative MFI of Ru(dpp)₃Cl₂ in different treatment groups, which corresponds to Fig. 3c3.

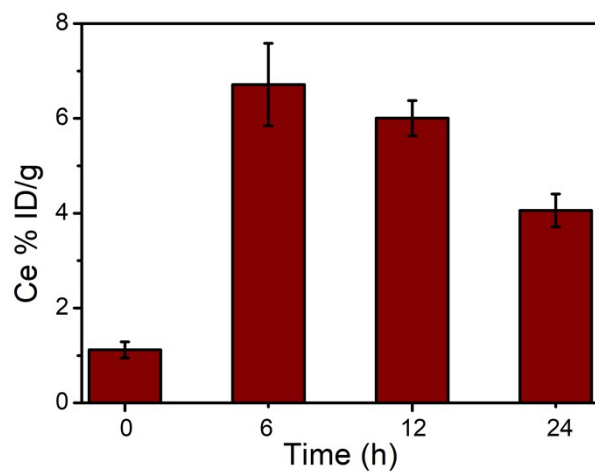


Fig. S25. Ce content in tumor tissues at different time points after the injection of SSA@Ce-HMSN-PEG.

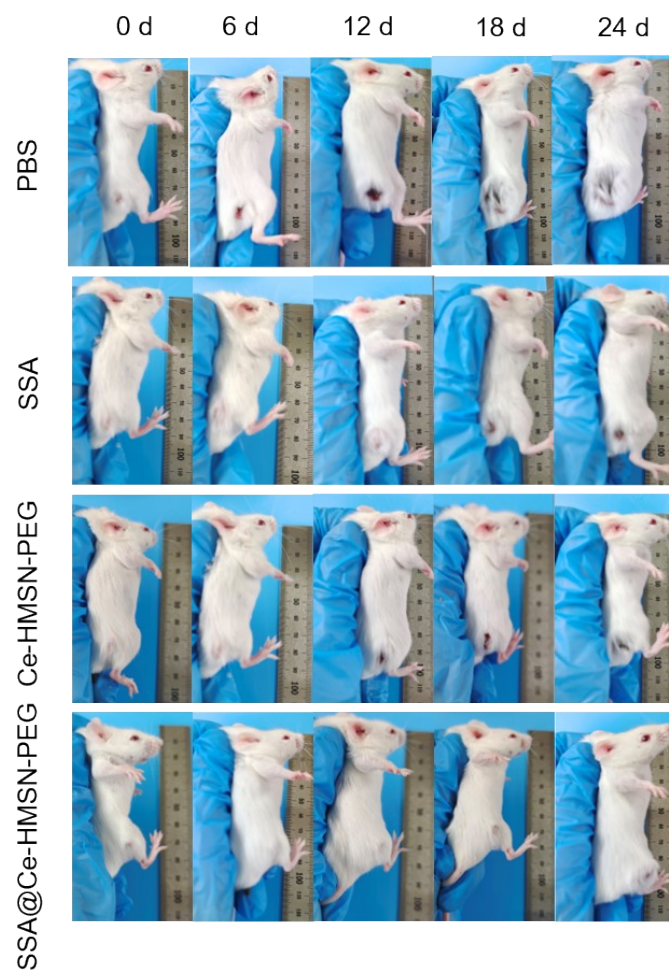


Fig. S26. Photos showing the tumor size in mice after different treatments.

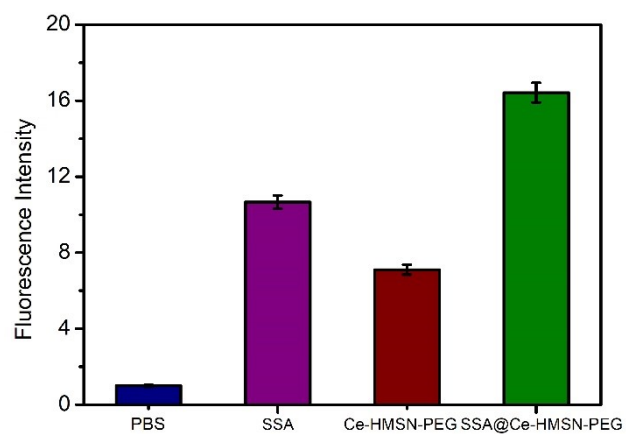


Fig. S27. Quantitative analysis of intracellular ROS levels from **Fig. 4e**.

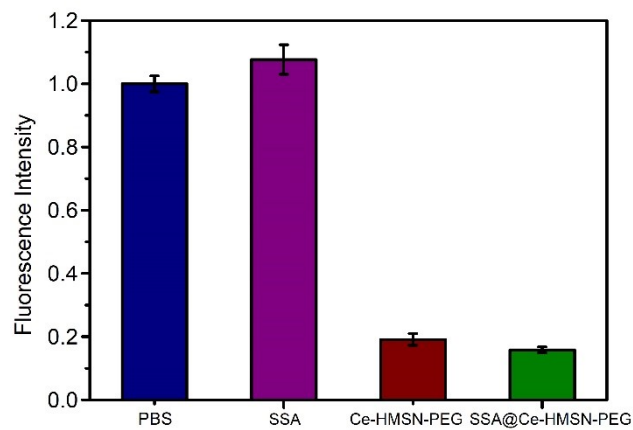


Fig. S28. Quantitative analysis of intracellular HIF-1 α level of tumor slices from **Fig. 4e**.

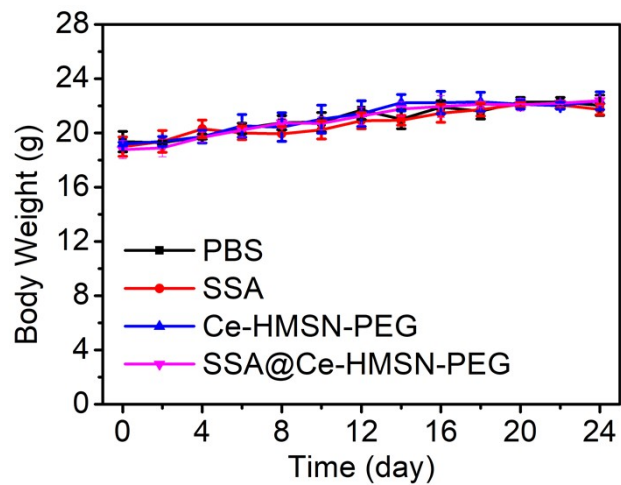


Fig. S29. Body weight curves of tumor-bearing mice with different treatments.

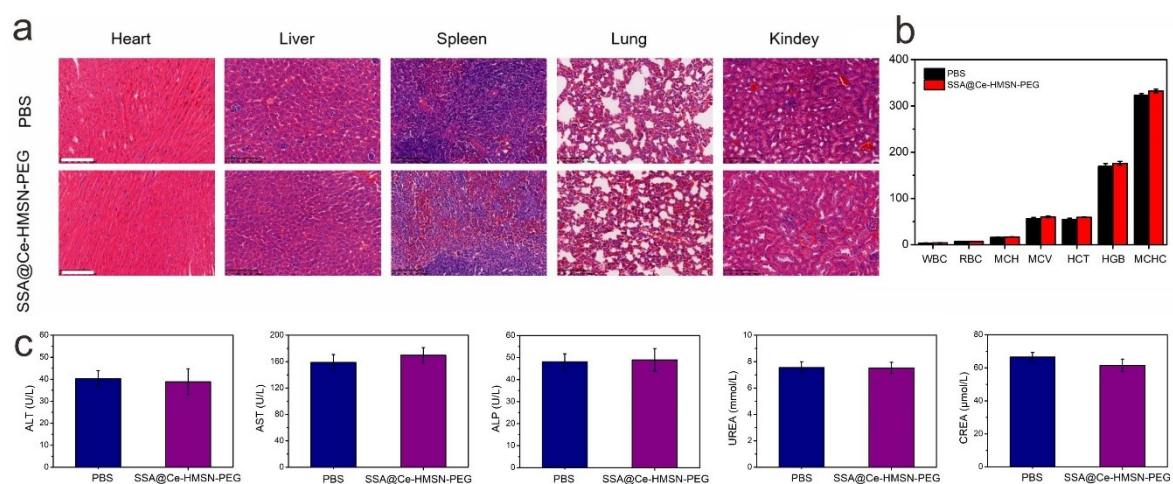


Fig. S30. Biocompatibility evaluation of SSA@Ce-HMSN-PEG. (a) Histological examination by H&E staining of major organs (heart, liver, spleen, lung and kidney) collected from tumor-bearing mice on 24th day. Scale bar: 100 μm. (b) Blood routine examination of tumor-bearing mice on the last day, which includes the results of white blood cell (WBC, 10⁹/L), red blood cell count (RBC, 10¹²/L), mean corpuscular hemoglobin (MCH, pg), mean corpuscular volume (MCV, fl), hematocrit (HCT, %), hemoglobin volume (HGB, g/L) and mean corpuscular hemoglobin concentration (MCHC, g/L). (c) Blood biochemical results including liver and kidney functions for PBS and SSA@Ce-HMSN-PEG groups: Alanine aminotransferase (ALT, U/L), aspartate aminotransferase (AST, U/L), alkaline phosphatase (ALP, U/L), urea (UREA, mmol/L) and creatinine (CREA, μmol/L).